Estimation of Land Surface Temperature of Pinder Watershed, Kumaun Himalaya Using Landsat-7 Data

N.C. Pant[1] J.S. Rawat[2] Meenaxi[3] Babita Negi[4]
[1,2,3,4]Department of Geography
[1]S.S.J. University, Almora, Uttarakhand, India [2,3]Kumaun University, Nainital, Uttarakhand, India
[4]H.N.B.G.U Uttarakhand, India

Abstract— Land Surface Temperature (LST) is one of the primary indices in the mechanics of land-surface processes on global and regional scales. It is the aggregation of the product of the terrain atmospheric interactions and energy fluctuation between the atmosphere and the terrain surface. Determining precisely the thermodynamics of LST is critical in huge range of applications such as climatology, hydrology, agriculture and biogeochemical and in change detection studies. The rapid advances in thermal remote sensing techniques have led to the measurement of LST from space borne applications in determining the impact of surface temperature dynamics at global, regional and local levels. The fundamental objective of the present paper is demonstration application of Remote Sensing techniques in determining of LST using one of the Great Himalaya watersheds of the Kumaun Himalaya, viz Pinder Watershed. For determining of the spatial distribution characteristics of surface temperature of Pinder watershed, the Landsat TM (Thermal Band) data of years 1990, 1999 and 2011 at a resolution of 30m are used. Mono-window and single channel algorithm were used to estimate land surface temperature for Pinder Watershed, and a correlation was made between LST, NDVI and Landuse/Land Cover (LU/LC) to analyses about land surface temperature and its distribution under different terrain categories by the application of GI Science techniques. The results reveals that the maximum, minimum and average temperature have increased from 21.65ºC, -17.50ºC, 2.07ºC to 26.07ºC, -9.03ºC, 8.52ºC respectively from 1990 to 2011.

Keywords: GI Science, Land Surface Temperature, Landsat TM (Thermal Band), NDVI, Landuse/Land Cover (LU/LC), Pinder Watershed

I. INTRODUCTION

LST is a key variable in climatological and environmental studies. Measurement of the surface temperature is a very important because it is essential for a huge range of application such as climatology, hydrology, agriculture, and biogeochemical also and in change detection studies (Wubet, 2003; Dash, 2005). Land surface temperature provides significant sequence regarding the surface physical processes and climate which play a major role in understanding several environmental problems (Dousset and Gourmelon 2003; Weng el at., 2004). LST which is controlled by surface energy balance, atmospheric state, thermal properties of the surface, and subsurface mediums, is an important and significant factor controlling most physical, chemical, and biological processes of the Earth (Becker and Li, 1990). LST has been shown to be an effective means of partitioning latent heat fluxes and thus surface radiant temperature response as a function of varying surface soil water content and vegetation cover (Owen et al., 1998). Estimation of LST from satellite thermal data, the digital number (N_D) of image pixels needs to be converted into spectral radiance using the sensor calibration data (Markham and Barker, 1986). However, the radiance converted from digital number does not represent a true surface temperature but a mixed signal or the sum of different fractions of energy.

II. STUDY AREA

The study area, viz., the Pinder Watershed (Figure 1) extends between 29°59′41″N to 30°18′57″N latitudes and 79°05′43″E to 80°04′38″E longitudes and encompasses an area of about 1872.98 km² in the Uttarakhand state in Central Himalaya, India. The altitude of the watershed varies between 757 m and 6746 m. The geographical distribution of snow cover reveals that in 1990 and 1999 about 9.40% (176.20 km^2) and 8.60% (161.08 km^2) area of the Pinder Watershed was under snow cover while in 2011 the snow cover was found 7.80% (147.50 km^2). These data suggest that due to global warming about 28.7 km^2 snow cover of Pinder Watershed has been converted into non-snow cover area at an average rate of 1.36 km²/year during the last two decades, i.e., in between 1990 to 2011(Pant el at., 2014).

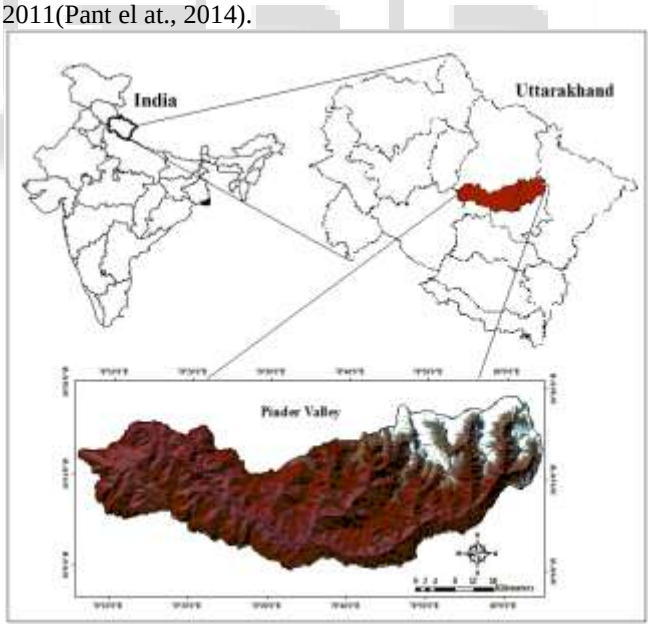

Fig. 1: Location map of the Pinder watershed, Central Himalaya (Uttarakhand).

III. METHODOLOGY

In this section a brief account of the methodology which was used for the study of LST of the study area is discussed. It includes description of data used, method of data processing and calculation of NDVI image and emissivity.

A. Data Used

Cloud free Landsat Satellite data of the years 1990, 1999 and 2011 for the study area has been downloaded from USGS

Earth Explorer website. All the data are pre-processed and projected to the Universal Transverse Mercator (UTM) projection system. The Landsat TM data of 1990, 1999 and 2011 are at a resolution of 30 m and are of same date and month i e. 15th November. These data used effectively for identification of the spatial distribution characteristics of surface temperature of Pinder watershed. The remote sensing data were processed using remote sensing software ERDAS imagine. Making a good mosaic requires some planning as their order can help to decide which images should overlay on others. ArcGIS's data management tools were used to make a mosaic data set to cover entire the study area.

B. Data Processing

The data processing chart (Fig. 2) depicts the data used and different steps of data processing for estimation of surface temperature from satellite data. The data processing done for the study area may be divided into four different phases there are:

1) Data Preparation,
2) Conversion from Digital Numbers to Spectral Radiance,
3) Conversion from Spectral Radiance to Temperature, and
4) Surface Temperature.

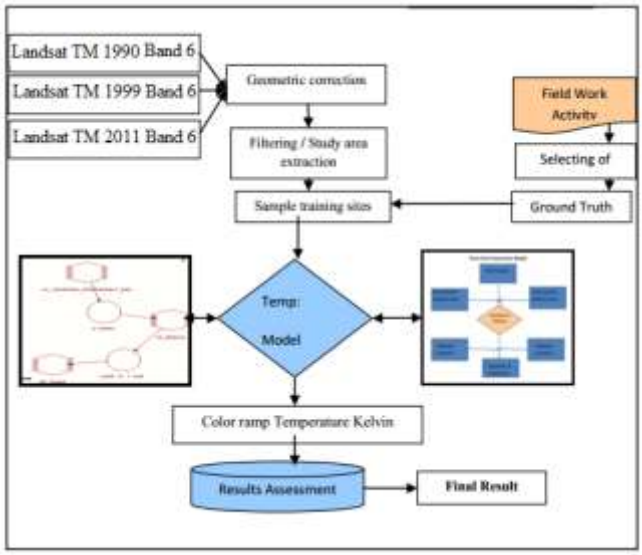

Fig. 2: Work Flow Chart showing the process of satellite data for Surface temperature estimation.

Map preparation Thermal band scenes were processed and analyzed using the ArcGIS software retrieved Spatial Analyst, one of the ESRI ArcView extensions. Band 6 of TM was analyzed for the determination of the surface temperatures. Images were compared with each other for understanding the relationship between the land cover types and different types of temperature in the Pinder watershed. Temperature Model was developed in the ERDAS Imagine for the calculation of the surface temperature. After completion of ERDAS imagine processing finally the images were opened in Arc Map software and color ramp scheme were applied, reflecting water bodies low temperature and dry land/ barren land in high temperature. The temperature values images are shown in Kelvin.

All objects having temperature above absolute zero (-273ºC) continuously emits EMR. In thermal remote sensing, sensors record this emitted or radiated energy instead of reflected energy. Therefore, in thermal remote sensing, the object itself is the source of energy. Although real objects do not behave as black bodies, this concept of black body is a convenient theoretical vehicle to describe the radiation principles of a material. The amount of radiation of a blackbody differs with the change of wavelength and its kinetic temperature. The amount of energy in object radiates in per unit area (considering all wavelengths) can be expressed by Stefan- Boltzmann laws (http://ijrsg.com/Files/IJRSG_16_07.pdf):

$$M = €T^4$$

Where, M= total radiant existence from the surface of a material, measured in W/M^2., €=Stefan-Boltzmann constant=$5.6697*10^{-8}$ $W/m^2/K^4$ and T= Temperature of emitting body measured in K.

The above equation tells us that doubling the absolute temperature of a body would render 16 times more radiation. The wavelength in which the maximum energy will be radiated or emitted is given by Wien's displacement law (http://ijrsg.com/Files/IJRSG_16_07.pdf):

$$€_{MAX} = b/T$$

Where, $€_{MAX}$= wavelength of maximum emitted energy, measured in µm., b=Wien's displacement constant= 2.897.7685 µm K and T = temperature of emitted body, measured in K. According to this law, for the sun, with a temperature of about 6000 K, the peak radiation is at 0.58 µm. The objects over the earth, as observed from the space by satellite, have peak radiation within 8-14 µm regions.

C. Spectral Radiance

For extraction of surface temperature from thermal band landsat, TM data are used. First the digital numbers (DNs) of the thermal band were converted in to spectral radiance. The digital number (DN) of band 3, 4 and 6 were converted to space reaching radiance or top-of-atmospheric (TOA) radiance at-sensor spectral radiance. Further, radiance is estimated using Landsat data with the following equation (http://ijrsg.com/Files/IJRSG_16_07.pdf):

$$L_\lambda = L_{min} + \frac{L_{max} - L_{min}}{255} \times DN \text{ (Band-6)}$$

Where, L_{min}=0.000 and L_{max}=17.040 are minimum and maximum of the radiance recorded by the Landsat-TM band 6.

D. Radiant Temperature

Thermal Infrared data (Band 6) of the Landsat TM were converted from spectral radiance (L) to radiant temperature (T_R) directly by the following equation (http://ijrsg.com/Files/IJRSG_16_07.pdf):

$$T(K) = \frac{k_2}{\ln\left(\frac{\epsilon k_1}{L_\lambda} + 1\right)}$$

Where, k_1= 666.09 K and k_2=1282.71 K.

Through above equation we find the temperature value of each pixel of the study area.

E. Kinetic Temperature

The radiant temperature (TR) was converted into kinetic temperature (TK) by using the following equation, (http://ijrsg.com/Files/IJRSG_16_07.pdf):

$$TK = \frac{TR}{\epsilon 1/4}$$

where, TK = kinetic temperature, TR = radiant temperature, and €= spectral emissivity.

F. Emissivity

Temperature and Emissivity Separation (TES) method (Gillespie and Rokugawa, 1998) has been used for deriving LST and emissivity estimations from five TIR bands (10–14μm) of ASTER data. TES products of surface emissivity (AST05) and land surface temperature (AST08) were acquired for comparison with those obtained by other algorithms.

Although several methods exist for the estimation of spectral emissivity, here we use NDVI (Normalized Different Vegetation Index). Calculation of the emissivity was done by using the following equation, (http://ijrsg.com/Files/IJRSG_16_07.pdf):

$$€= a + b \times \ln(NDVI)$$

where, € and NDVI are average thermal emissivity and average normalized difference vegetation index for individual surface covers respectively, a and b are two constants (a = 1.0094 and b = 0.047 for a correlation coefficient of 0.941 at 0.01 level of significance).

Emissivity information is required to convert brightness temperature to kinetic surface temperature. As mentioned previously, there are several methods to retrieve surface emissivity. Based on the NDVI values of different land use classes, emissivity image was prepared by assigning emissivity. Since Landsat has only a single window for thermal data, it is impossible to obtain emissivity directly for TM/ETM data without using other spectral bands. One technique for estimating emissivity that can be applied is a fractional cover mixture model. It is assumed that the soil background and the vegetation have specific known emissivities and that they ‘‘mix’’ according to the fractional cover (Sobrino et al., 2001). The fractional vegetation cover is then estimated from the NDVI. Some investigators have also established empirical models between NDVI and emissivity (Valor and Caselles 1996) values as 0.90 for built up area and 0.98 for vegetation. Emissivity estimated based upon fractional vegetation cover could not be directly evaluated with ground-based observations. However, we were able to compare these estimates with those derived using multi-channel band thermal-IR data. It should be noted that it is difficult if not impossible to judge which method is more reliable without more information or a data set where there is great variation in emissivity. The emissivity image for the study area was prepared for 1990, 1999 and 2011 which is presented in figure 3. Emissivity has been widely used as an indicator of nature of the surface and temperature. The emissivity values estimated are in the range of 1.00 to 0.75 in 1990, while in 1999 emissivity range was estimated 0.99 to 0.71 and in 2011 the emissivity values estimate is in the range of 1.00 to 0.71.

G. Normalized Different Vegetation Index (NDVI)

Its measures the greenness of the environment and the amount of vegetation. The NDVI is computed form the following equation (http://ijrsg.com/Files/IJRSG_16_07.pdf).

$$NDVI = \frac{band_{NIR} - band_{RED}}{band_{NIR} + band_{RED}}$$

where, NIR is the near infrared radiance from band 4 and RED is the red radiance from band 3 of landsat TM.

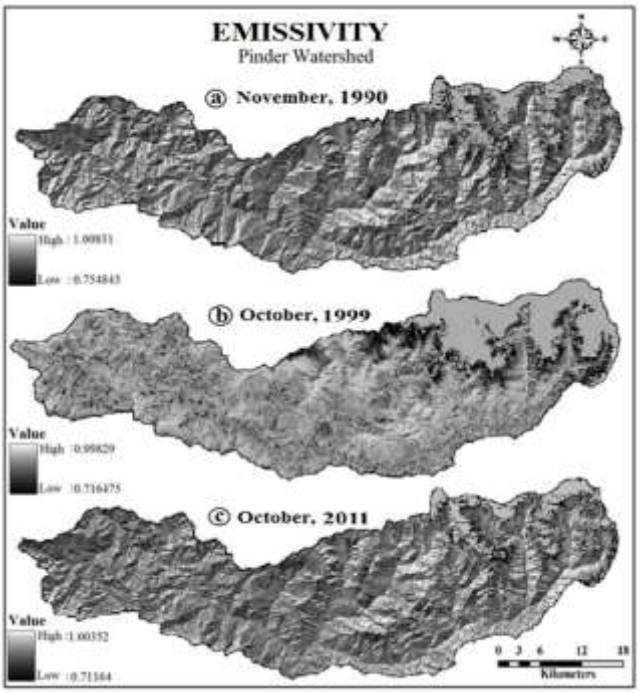

Fig. 3: Emissivity of different years in the Pinder watershed; (a)1990, (b) 1999 and (c) 2011, (Based on Landset data).

The Normalized Difference Vegetation Index (NDVI) is one of the most widely used index of which applicability in satellite analysis and in monitoring of vegetation cover has been sufficiently verified in the last two decades. The NDVI value of the pixels varies between -1 and +1. Higher values of NDVI indicate the richer and healthier vegetation. Vegetation affects the latent thermo flux of the surface intent to the atmosphere through the evapotranspiration. Lower Land Surface Temperature (except water bodies) is usually measured in areas with higher NDVI values.

The NDVI is a measure of the amount and vigour of vegetation at the surface. The reason NDVI is related to vegetation is that healthy vegetation reflects very well in the near infrared part of the spectrum. Green leaves have a reflectance of 20% or less in the 0.5 to 0.7 range (green to red) and about 60% in the 0.7 to 1.3 μm range (near infrared). The value is then normalized to -1<=NDVI<=1 to partially account for differences in illumination and surface slope. The NDVI image developed for the present study area for the year 1990, 1991 and 2011 is shown in the figure 4. NDVI has been widely used as an indicator of vegetation abundance to estimate LST. The NDVI values estimated are in the range of 0.739 to -0.8 in 1990, while in 1999 NDVI range was estimated 0.789 to -0.942 and in 2011 the NDVI values estimated are in the range of 0.747 to -0.5.

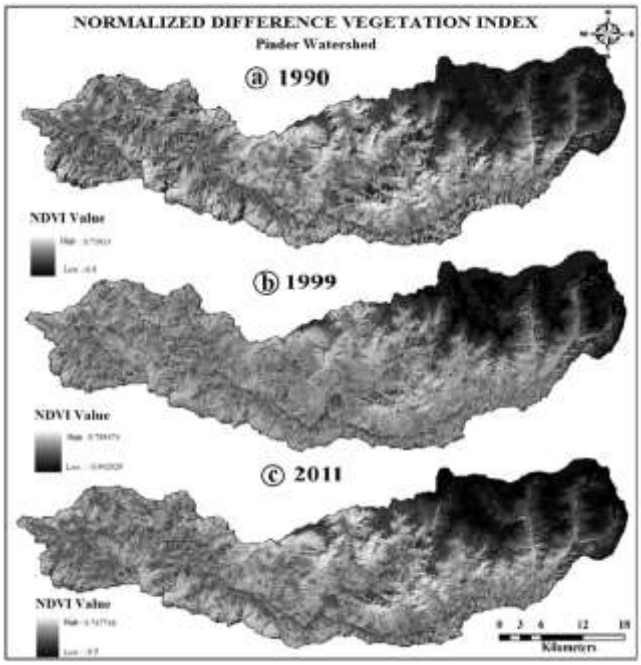

Fig. 4: Geographical distribution of NDVI value in different years in the Pinder watershed; 1990, (b) 1999 and (c) 2011 (based on Landset data).

IV. RESULT AND DISCUSSION

A. Distribution of LST

Figure 5 depicts the distribution of surface temperature in the Pinder watershed in different years, i.e., 1990, 1991, 2011. A brief description of temperature description is presented in following paragraphs

In November, 1990 the high temperature of Pinder watershed was found 21.65 ºC and low temperature was (-)17.50 ºC. Table 1 reveals that the average temperature of the watershed was about 2.07^{0}C in the month of November 1990. Table 1 reveals that in the month of October, 1999 the high temperature of Pinder watershed was 23.94 ºC while the low temperature was (-)13.28ºC. The average temperature of the Pinder watershed was 5.33ºC in the month of October, 1999. In October, 2011 the high temperature of Pinder watershed was 26.07ºC and low temperature was (-)9.03ºC. Table 1 reveals that the average temperature of the Pinder watershed was 8.52ºC in the month of October, 2011.

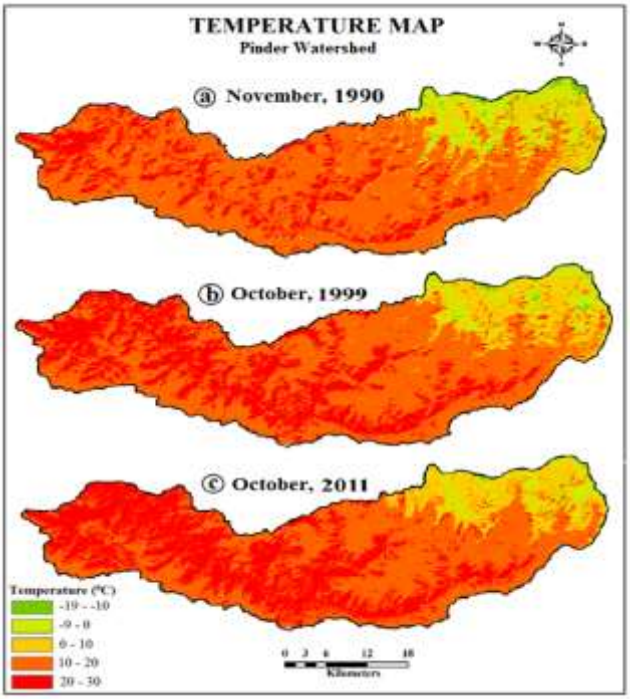

Fig. 5: Land surface temperature in different years in the Pinder watershed; (a) 1990, (b) 1999 and (c) 2011, (based on Landset data).

Years	Temperature (ºC)			Change (ºC)		
	High	Low	Average	High	Low	Average
November, 1990	21.65	-17.50	2.07	-	-	-
October, 1999	23.94	-13.28	5.33	2.29	4.22	3.26
October, 2011	26.07	-9.03	8.52	2.13	4.25	3.19
Nov,1990 to Oct, 2011	23.89	-13.27	5.3	4.42	8.47	6.45

Table 1: Land surface temperature in Different Years in the Pinder watershed.

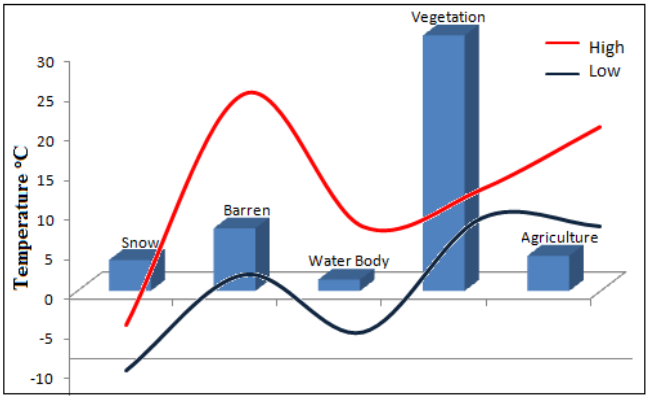

Fig 6: Land surface temperature in different Lend use category in Pinder Watershed.

Land cover Categories	Area km^2	Temperature (^{0}C)		
		High	Low	Average
Snow	147.50	-3.18	-9.03	-6.10
Barren	299.03	26.04	3.12	14.58
Water Body	53.87	9.26	-4.18	2.54
Vegetation	1221.35	13.96	10.26	12.11
Agriculture	168.18	21.84	9.23	15.53

Table 2: Land surface temperature classification of different land cover categories in the Pinder watershed in 2011.

The LST obtain for the study area using above methods and techniques in present figure 5 which depicts spatial distribution of LST in different years ie., 1990, 1999, 2011. The results are summarized in table 1. The result of LST in different lend use/ lend cover is summarized in table 2 and diametrical illustration if figure 6. A brief account of above result in deceased in the following paragraph.

V. LST UNDER DIFFERENT LAND USE/ LAND COVER

Figure 6 and Table 2 shows the estimated surface temperature values over different Land use and land cover category. The values are maximum for barren land ranging from 26.04 to 3.12 °C (Average of 14.58°C) and minimum over snow cover area ranging from (-)3.18 to (-)9.03°C (Average of -6.10°C). Vegetation has low temperature because the amount of heat stored is reduced through transpiration. The impact of snow cover is clearly seen as low temperature values. The relationship between surface radiant temperature of land-cover is influenced by land-use in Pinder watershed.

In the research the potential of remote sensing to study the Land surface temperature is presented by estimating the spatial distribution and intensities of Land surface temperature. Emissivity and surface temperature enables in better understanding of the overall watershed area. Land surface temperature for the study area was generated using Landst Data (6 Bands) of different years. Mono-window and single channel algorithm were used to estimate land surface temperature for Pinder watershed. Emissivity was calculated using NDVI and supervised classification method of Land use/Land cover. land surface temperature was compared with in situ and the result showed a positive correlation with NDVI and Land use/Land cover method. NDVI was obtained for three different years (1990, 1999 and 2011) for Pinder watershed. Using NDVI Index threshold technique land surface temperature was derived. The output of land surface temperature was compared with the NDVI output and a positive correlation was found in between them. From brightness, temperature and emissivity images, the final Land Surface Temperature image was obtained by developing a model in the ERDAS Imagine 9.1.

The above result are based on remote sensing data, i,e., Landsat TM (Thermal Band). Therefore, the study demonstrates that remote sensing and GIS technologies are very useful for studying land surface temperature distribution under different land use categories. The results reveals that the maximum, minimum and average temperature have increased from 21.65^{o}C, -17.50^{o}C, 2.07^{o}C to 26.07^{o}C, -9.03^{o}C, 8.52^{o}C respectively from 1990 to 2011. In 1990 the maximum, minimum and average temperature were 21.65^{o}C, -17.50^{o}C, 2.07^{o}C which increased to 23.94^{o}C, -13.28^{o}C, 5.33^{o}C with the change rate 2.29^{o}C, 4.22^{o}C, 3.26^{o}C respectively in 1999. The maximum, minimum and average temperature were 23.94^{o}C, -13.28^{o}C, 5.33^{o}C in 1999 which increased 26.07^{o}C, -9.03^{o}C 8.52^{o}C to with the change rate 2.13^{o}C, 4.25^{o}C, 3.19^{o}C respectively in 2011.

REFERENCES

[1] Becker, F. and Li. Z.L. (1990): Towards a local split window metho over land surfaces, Int. J. Remote Sensing, Vol. 11, pp. 369-393.
[2] Dash, P. (2005): Land surface temperature and emissivity retrieval from satellite measurements, PhD thesis, Institute for Meteorology and Klimaforschung, pp. 1-3.
[3] Dousset, B. and Gourmelon, F. (2003): Satellite multi-sensor data analysis of urban surface temperatures and land cover, ISPRS Journal of Photogrammetric and Remote Sensing, Vol. 58, pp. 43-54.
[4] Markham, B. L. and. Barker. J. L. (1986): Landsat MSS and TM post-calibration dynamic rangers, exoatmospheric reflectance and at-satellite temperatures, EOSAT Landsat Tech. Notes (Aug.), pp. 3-8.
[5] Owen, T.W., Carlson, T.N. and Gillies, R.R. (1998): Remotely sensed surface parameters governing urban climate change, Internal Journal of Remote Sensing, Vol. 19, pp. 1663- 1681.
[6] Pant, N.C., Kumar, M., Rawat J.S. and Rani, N. (2014): Study of Snow Cover Dynamics of Pinder Watershed in Central Himalaya using Remote Sensing and GIS Techniques, Vol. 3 pp. 122-128.
[7] Sobrino, J.A., Raissouni, N. and Li, Z. (2001): A comparative study of lan surface emissivity retrival from NOAA data.Remote Sensing of Environment, Vol. 75, pp. 256–266.
[8] Valor, E. and Caselles, V. (1996): Mapping land surface emissivity from NDVI: Application to European, African, and South American areas. Remote Sensing of Environment, Vol. 57, pp. 167–184.
[9] Weng, Q., Lu, D. and Schubring, J. (2004): Estimation of land surface temperature-vegetation abundance relationship for urban heat island studies, Remote Sensing of Environment, Vol. 89 (4): 467-483.
[10] Wubet, M.T. (2003): Estimation of absolute surface temperature by satellite remote sensing, Unpublished M.Sc Thesis, International Institute for Geoinformation Science and Earth Observation, Netherlands.

